

Structural Properties of CrF₃- and MnCl₂-Filled Poly(vinyl alcohol) Films

H. M. Zidan

Physics Department, Faculty of Science at Damietta, Mansoura University, P.O. Box 34517, New Damietta, Egypt

Received 10 September 2001; accepted 24 February 2002

Published online 18 February 2003 in Wiley InterScience (www.interscience.wiley.com). DOI 10.1002/app.12123

ABSTRACT: Poly(vinyl alcohol) (PVA) films filled with different amounts of CrF₃ and MnCl₂ were prepared by the casting method. Differential scanning calorimetry (DSC) and X-ray diffraction (XRD) analysis were used to study the changes in the structure properties that occurred because of filling. The changes occurring in the measured parameters with increasing filler contents were interpreted in terms of the structural modification of the PVA matrix. All the studied samples had a main melting temperature due to the main crystalline phase of PVA. The intensity and position of this peak depended on the filling level. However, the samples of CrF₃-filled PVA films with a filling level greater than

or equal to 10 wt % revealed another melting temperature, which indicated the presence of a new crystalline phase in addition to the main crystalline phase. The changes that occurred in the degree of crystallinity of the studied samples were examined. The calculated degree of crystallinity was formulated numerically to be an exponential function of the filling level. The XRD patterns of the studied samples confirmed the DSC results. © 2003 Wiley Periodicals, Inc. *J Appl Polym Sci* 88: 1115–1120, 2003

Key words: X-ray; differential scanning calorimetry (DSC); structure

INTRODUCTION

Metal-halide-doped polymers have been the subject of both theoretical and experimental studies because of their increasing technological importance. Doping polymers with transition-metal halides has a significant effect on their physical properties. The changes in the physical properties of the polymers due to doping depend on the chemical nature of the doping substances and the ways in which they interact with the host matrix.^{1–3} One may select a suitable type and doping level of a transition-metal halide to prepare a doped polymer with a desired physical property.⁴

Poly(vinyl alcohol) (PVA) is a nontoxic, water-soluble synthetic polymer that is widely used in biochemical and medical applications because of its compatibility with the living body.⁵ Water-soluble PVA is rendered insoluble by the introduction of crosslinks. PVA has good film-forming and highly hydrophilic properties and has been studied as a membrane in various ways. PVA has recently been exploited as a substrate for enzyme immobilization in the form of photocrosslinkable PVA.⁶ PVA gels can be prepared from aqueous solutions by repetitive freezing and throwing.⁷

A film obtained by the casting of an aqueous PVA solution has a 100% amorphous structure. PVA hydrogels prepared by the freezing of a concentrated aqueous PVA solution exhibit, however, a diffraction pat-

tern from the (101) spacing corresponding to 4.55 Å.⁸ An important feature of the semicrystalline PVA polymer is the presence of crystalline and amorphous regions. The two regions are well separated by portions of an intermediate degree of ordering, which enhances the macromolecule, producing several crystalline and amorphous phases.

A crystalline polymer may be regarded as an amorphous matrix in which small crystallites are randomly distributed. However, it is more natural to treat a crystalline polymer as a certain sufficiently imperfect crystalline lattice in which voids are filled with amorphous matter.⁹ The role of amorphous regions may be played by sites saturated with crystal defects, which form chain-folded crystals. The importance of the semicrystalline PVA polymer arises from the role of the OH group and the hydrogen bond.¹⁰

The physical properties of PVA doped with some transition-metal salts were investigated.^{11–13} In this work, we studied the effect of both the filler concentration [or filling level (*W*)] and the nature of the metal halides on the structure modification of PVA films.

EXPERIMENTAL

Sample preparation

The PVA and metal halides used in this work were supplied by Aldrich Chemical Co. These PVA films, with different amounts of chromium fluoride (CrF₃) and manganese chloride (MnCl₂), were prepared by the casting method as follows.¹¹ PVA powder was

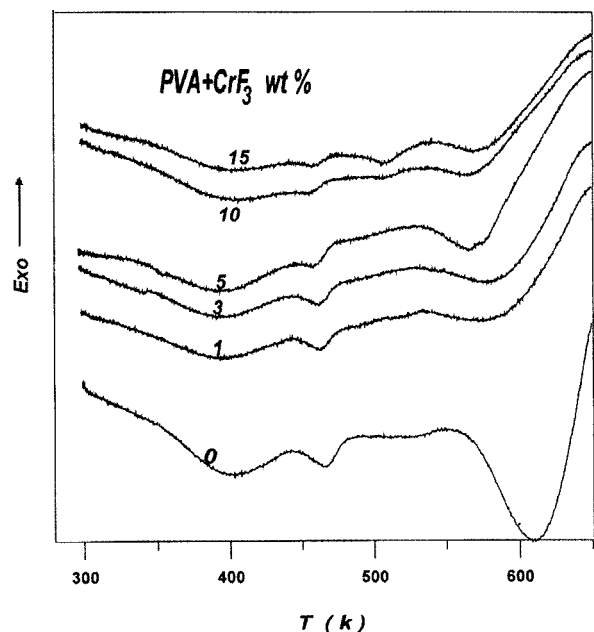


Figure 1 DSC curves for PVA films with different W values of CrF_3 .

dissolved in distilled water and then heated gently, with a water bath, for complete dissolution. CrF_3 or MnCl_2 was also dissolved in distilled water and added to the polymeric solution. The solutions were left to reach a suitable viscosity, after which they were cast into glass dishes and left to dry in a dry atmosphere at room temperature. Samples were transferred to an electric air oven held at 60°C for 48 h for the minimization of the residual solvent. The thickness of the obtained films was 0.1–0.2 mm. PVA films filled with CrF_3 mass fractions of 0, 1, 3, 5, 10, and 15% and PVA films filled with MnCl_2 mass fractions of 0, 10, 15, 20, 25, 35, and 40% were prepared. W (wt %) was calculated as follows:

$$W \text{ (wt \%)} = \frac{w_f}{w_p + w_f} \times 100 \quad (1)$$

where w_f and w_p represent the weights of the filler and polymer, respectively.

Physical measurements

Differential scanning calorimetry (DSC)

The thermal analysis of PVA films filled with different mass fractions of metal halides was performed via DSC with a Stanton Redcroft model DTA 673-4 apparatus. A heating cycle was made from room temperature to 650 K with a programmed heating range of 10 K/min. The values of the glass-transition temperature (T_g) and melting temperature (T_m) were obtained. The change in the degree of crystallinity (X) was detected

by the calculation of the endothermic thermogram area of DSC.

X-ray diffraction (XRD)

XRD diagrams of the studied samples were recorded with a Philips PW 1050/80 diffractometer. Ni-filtered $\text{Cu K}\alpha$ radiation generated 30 kV and 30 mA. The radiation was incident on the sample, which was scanned at $1^\circ/\text{min}$ over a range of $2\theta = 5\text{--}40^\circ$.

RESULTS AND DISCUSSION

DSC

The thermal behavior of PVA films filled with different fractions of CrF_3 was studied with DSC from 298 to 630 K (Fig. 1). The pure PVA films displayed three transitions at 351, 443, and 467 K in addition to another endothermic peak at 610 K, which indicated the thermal degradation of the polymer. These transitions could be interpreted as follows.^{5,13,14} The transition at about 351 K was attributed to the T_g relaxation process resulting from micro-Brownian motion of the main-chain backbone. The exothermic peak at about 443 K was broad and shallow and was attributed to the α relaxation associated with the crystalline region. The endothermic peak at 467 K was attributed to T_m of pure PVA.

It can be observed in Figure 1 that the thermal behavior of the PVA films filled with mass fractions of less than 10 wt % CrF_3 was similar to that of the pure PVA films. The magnitude of the thermal degradation temperature (T_D) of pure PVA was greater than those of the filled samples (Table I). It is suggested that the addition of CrF_3 to the PVA films reduced the thermal stability. The position of T_g for PVA films filled with different amounts of CrF_3 was shifted slightly toward lower temperatures with respect to the unfilled film (Table I). This also suggests that the segmental mobility of amorphous pure PVA increased because of the addition of CrF_3 and that the PVA segments became less rigid. This indicates that the CrF_3 filler acted as plasticizer. Increasing the CrF_3 content resulted in a decrease in both T_g and T_D of the PVA films; therefore, the CrF_3 molecules greatly affected the PVA structure.

TABLE I
Transition Temperatures of the DSC Thermograms for PVA Films Filled with Different Levels of CrF_3

W (wt%)	T_g (K)	T_α (K)	T_p (K)	T_{m1} (K)	T_{m2} (K)
0	351	398	610	467	—
1	350	399	590	463	—
3	347	400	583	460	—
5	346	403	572	457	—
10	345	405	571	456	508
15	344	406	570	455	509

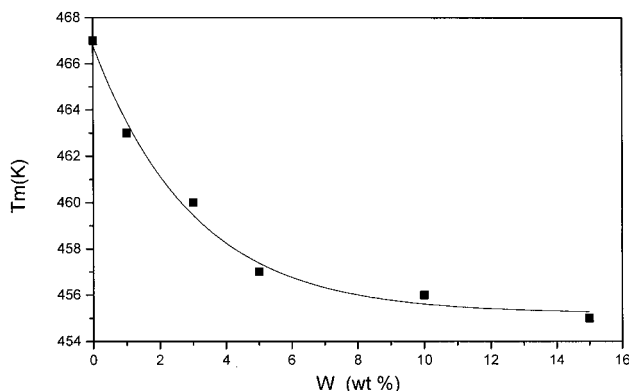


Figure 2 W dependence of T_m of CrF_3 -filled PVA films.

With respect to the α -relaxation temperature (T_α) for PVA films filled with different amounts of CrF_3 , it is shown in Figure 1 that the value of T_α slightly increased and its peak intensity decreased with increasing W values of CrF_3 . The change in the position of T_α might mainly have been due to the effect of filling on the orientation of the crystals, crystallinity, and microstructure of the sample. It is known that the changes in the crystalline structure and morphology affect the magnitude and position of the α relaxation in PVA.¹⁵ It was expected that T_α could be influenced by the size and perfection of the crystals and, therefore, their T_m values. The magnitude of the relaxation might have been affected by the orientation of the crystals and the crystallinity and microstructure of the sample. If the α relaxation in PVA was associated with a particular movement, its intensity would have varied with the crystal orientation. Therefore, if the motions were perpendicular to the chain axis, the detected magnitude of the transition would have decreased as the orientation of the crystals along the chain axis increased. Also, the α -relaxation magnitude depended on the density and perfection of the crystal packing.¹⁶ However, Popli et al.¹⁷ measured T_α of polyethylene (PE) samples by dynamic mechanical analysis at 3.5 Hz. They reported that T_α depended on the crystal thickness.

A reduction in the T_m values of PVA crystals was evident with an increase in W of CrF_3 (Table I). This behavior is illustrated in Figure 2, in which T_m is plotted against W of CrF_3 . The distribution of T_m was converted into a distribution of the crystallite thickness with the Thomson–Gibbs equation:¹⁸

$$T_m = T_m^0 \left(1 - \frac{2\sigma_e}{\Delta H L} \right) \quad (2)$$

where T_m is the observed melting temperature of a crystal of lamellar thickness L , T_m^0 is the equilibrium melting temperature of an infinitely thick crystal, σ_e is the surface area of the chain folds, and ΔH is the heat

TABLE II
Calculated Values of Crystal Lamellar Thicknesses of PVA Films Filled with Different Levels of CrF_3 Calculated with the Thomson–Gibbs Equation

W (wt %)	0	1	3	5	10	15
Crystallite thickness (Å)	96	86	80	74	72	71

of fusion per unit volume of the crystals. The value of $\sigma_e/\Delta H$ used for PVA was 3.3×10^{-8} cm, and T_m^0 was 501.5 K.¹⁴ The calculated values of the crystal lamellar thickness (Table II) imply that the crystal structure of the PVA films filled with different contents of CrF_3 was basically different from that of the ordinarily obtained PVA films. The endotherm of the T_m form became less sharp with increasing CrF_3 , and this indicated the decreases in the size of the crystallite and/or the order of molecular packing in the crystallite.

The heat required for melting the sample (ΔH) was obtained by the integration of the area under the melting peak. Figure 3 shows the variations of ΔH for PVA films filled with different amounts of CrF_3 (W). The ΔH values decreased exponentially with an increasing CrF_3 W value. This can be interpreted if we consider that CrF_3 molecules induce defects in a crystalline phase in PVA. These results suggest the following numerical formula for the dependence of ΔH on W :

$$\Delta H = \Delta H_0 + A \exp(-W/B) \quad (3)$$

where ΔH_0 , A , and B are constants. This variation of ΔH could be attributed mainly to the variation of X .¹⁹ This is clarified in the XRD section of this work.

For films with W values of CrF_3 greater than or equal to 10 wt %, an additional melting peak appeared at the higher temperature side of the ordinary peak (Fig. 1). The endotherm of the high T_m form became sharper with an increasing amount of CrF_3 , and this

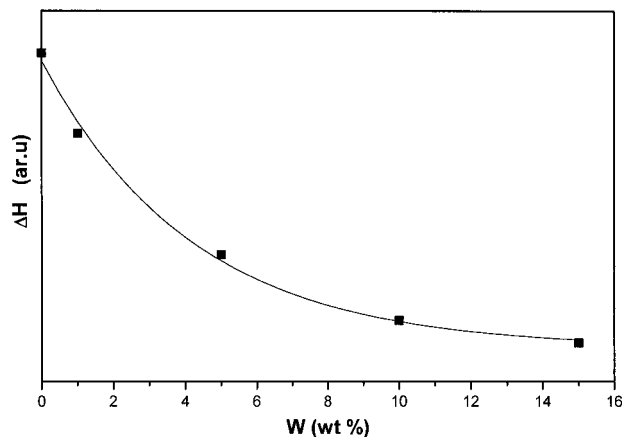


Figure 3 W dependence of ΔH of CrF_3 -filled PVA films.

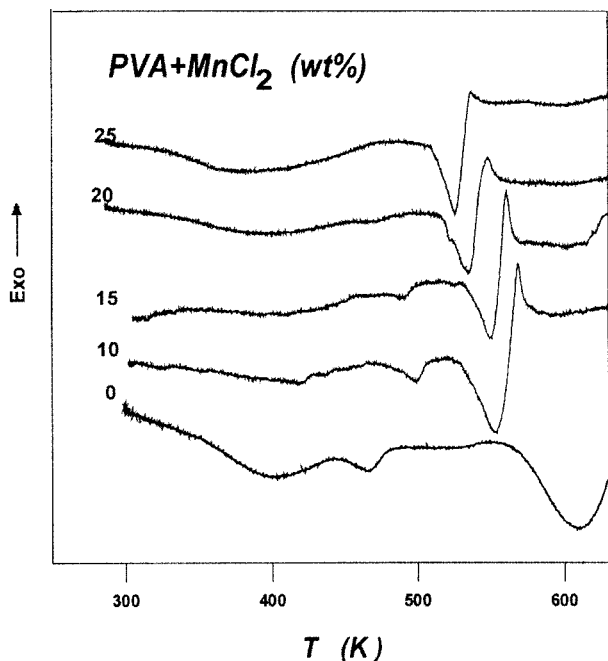


Figure 4 DSC curves for PVA films with different W values of MnCl_2 .

indicated an increase in the size of the crystallite and/or the order of molecular packing in the crystallites. Such two-peak melting curves were reported by Cha et al.²⁰ The two endotherms of their DSC curves for highly drawn PVA fibers were clearly separated peaks. The high T_m form is thought to be another kind of crystallite. Also, the DSC curves of drawn special PVA films after aging for more than 30 days showed another melting peak at the higher temperature side of the ordinary peak.²¹

A fusion curve with dual or multiple peaks has often been reported also for other polymers such as polyethylene²² and nylon 66,²³ together with abnormally high T_m values, when the polymers are crystallized at very high pressures or under conditions giving rise to high molecular orientation. The structure and physicochemical properties of PVA films were studied when they were stretched in the amorphous state and annealed.²⁴ The PVA films showed a dual fusion curve and a very high T_m . Therefore, the dual fusion curve and the high T_m seem to be general characteristics of polymers crystallized under conditions inducing high molecular orientation, regardless of the polymer type. This dual peak strongly indicates the presence of a dual structure or a very high ordered crystalline phase of large dimensions, in addition to the normal crystalline region.

The thermal behavior of PVA films filled with different amounts of MnCl_2 was observed with DSC (Fig. 4). This figure shows no major changes from the general shape of the DSC curves of PVA films filled with CrF_3 . For MnCl_2 , there was one melting peak, its area

decreased with increasing W , and the peak disappeared at $W \geq 25$ wt %. This indicated that the main crystalline phase decreased with increasing W and that the samples became completely amorphous for $W \geq 25$ %. Also, another crystalline phase did not form as for CrF_3 , although in this case we used high concentrations of MnCl_2 . In Figure 4, we see also that T_m increased with increasing MnCl_2 content, although usually this value decreases with decreasing X . This result was very unusual, and the discrepancy suggested that the crystallites of PVA were more highly organized in the filled films than in the pure PVA homopolymer; that is, there was an increase in the crystallite size (V) and there was a difference in the density between the crystalline and amorphous regions.

V was calculated from Sherrer's equation²⁵ with a (101) plane:

$$V_{hkl} = \frac{R\lambda}{\beta \cos \theta} \quad (4)$$

where hkl is the index of the plane, R is 1, λ is 1.54 Å, and β is the half-width of the 101 plane. Figure 4 shows that β decreased with an increasing amount of MnCl_2 . This means that V for PVA increased with an increasing content of MnCl_2 . This result supports the previous discussion.

XRD

Figure 5 displays the XRD scans of pure PVA and PVA containing different levels of CrF_3 . It is obvious that there was no significant effect on the general shape of the X-ray pattern. The observed spectra characterize a semicrystalline polymer possessing a clear crystalline peak for all the studied samples at a scattering angle of $2\theta \cong 19.2^\circ$, corresponding to a (101) spacing.²⁶ A reduction in the area under the crystalline peak or its height is evidence of the increase in the CrF_3 content. It is known that the area under the crystalline peak or its height can be taken as a measure of X . The calculated values of the height of the main peak (101) are plotted as a function of W of CrF_3 in Figure 6. The peak height decreased exponentially with increasing W . This means that X decreased exponentially because of the addition of CrF_3 . X depended on W according to the following formula:

$$X = X_0 + A_1 \exp(-W/B_1) \quad (5)$$

where X_0 , A_1 , and B_1 are constants. From eqs. (3) and (5), we can see the similarity of the W dependence of ΔH and the corresponding dependence for the crystalline peak height. Also, X may be considered to be an indicator for W .

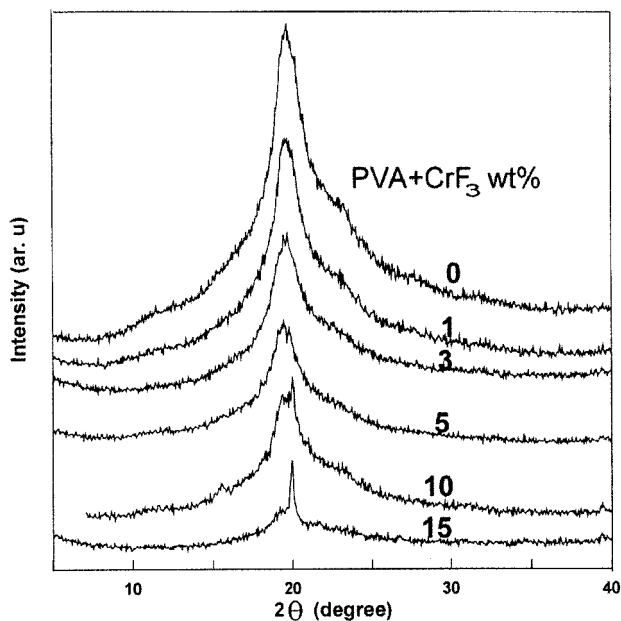


Figure 5 XRD scans of PVA films with various W values of CrF_3 .

It is remarkable that, in Figure 5, for samples containing 10 and 15 wt % CrF_3 , there is a sharp peak superimposed on the main peak at $2\theta = 20.2^\circ$. This peak belongs to neither PVA nor CrF_3 crystalline spectra, but it may arise from scattering atomic planes of some crystalline patterns of the PVA- Cr^{3+} complex. The appearance of two T_m 's (T_{m1} and T_{m2}) in the DSC scans for W values of CrF_3 greater than or equal to 10 supports the existence of two crystalline phases. The first crystalline phase was the main phase of PVA, which decreased with increasing CrF_3 content because of the induced defects, and the second crystalline phase characterized the PVA- Cr^{3+} complex. Similar results²⁷ were observed for PVA filled with 5 wt % CrCl_3 irradiated by low-level fast neutrons. It was reported that the addition of CrCl_3 to PVA could cause structural variations in the polymeric network. These

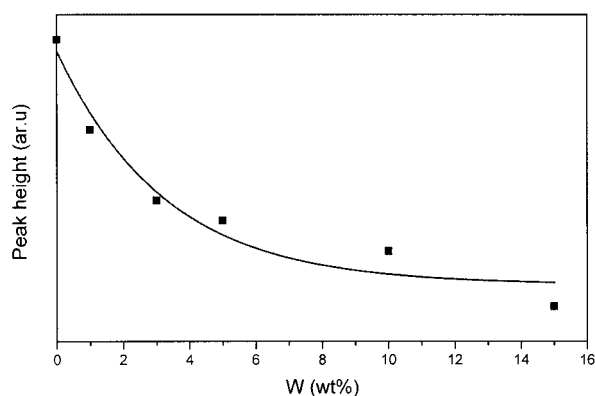


Figure 6 W dependence of the height of the main peak in the XRD patterns of CrF_3 -filled PVA films.

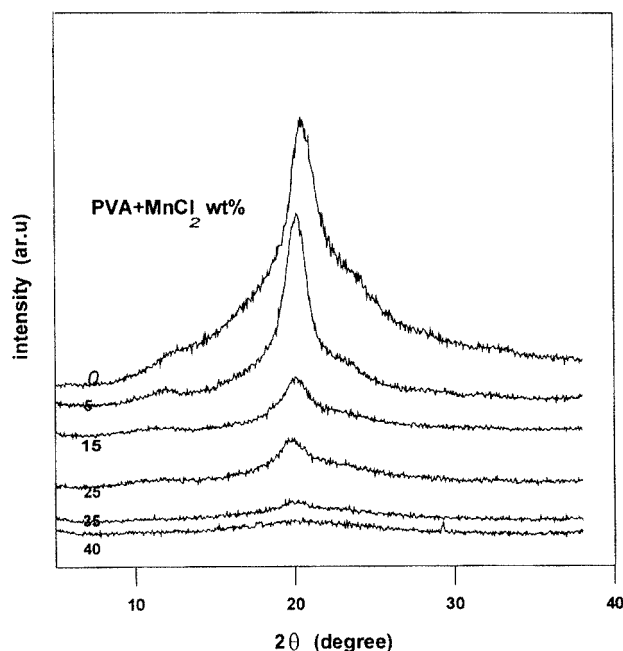


Figure 7 XRD scans of PVA films with various W values of MnCl_2 .

variations were most likely related to the interactions between the negatively charged hydroxyl groups and positive chromium ions.

Figure 7 provides the XRD patterns for PVA filled with different levels of MnCl_2 . The main peak did not change in shape or position, but the intensity of the main peak decreased exponentially with increasing W . The W dependencies of the height of the main peak (101) for MnCl_2 -filled PVA films was similar to that for CrF_3 -filled PVA films (figure not shown). At high concentrations ($W \geq 35$), the filled PVA films became completely amorphous. Das et al.²⁸ measured X-ray diagrams for PVA and fluorinated PVA. They reported that PVA became highly amorphous after fluorination. Although PVA is atactic, it possesses a certain regularity in its virgin state. However, on fluorination, its crystalline order is lost because of the incorporation of fluorine and unsaturation. Referring to Figure 7, one can observe that no new crystalline phases appeared because of filling with MnCl_2 , contrary to filling with CrF_3 . The appearance of one melting peak in the DSC scans, its area decreasing with an increasing content of MnCl_2 and disappearing at high concentrations, confirmed these results. This means that the structural modifications depended on W and the nature of the filler. We obtained PVA films with desired crystallinity by the addition of MnCl_2 at certain levels. Also, we obtained amorphous PVA films with the addition of MnCl_2 with $W \geq 25$ wt %. However, PVA films were obtained with a dual crystalline phase with CrF_3 with $W \geq 10$ wt %.

CONCLUSIONS

From an analysis of DSC curves and XRD patterns of filled PVA films, it may be said that the structure changes took place after the filling with CrF_3 and MnCl_2 as a result of defect formation. From the DSC curves, we noticed the following: (1) an increasing filler content resulted in a decrease in both T_g and T_D of PVA films, which indicated that the filler acted as a plasticizer; (2) for all the investigated samples, there was a main melting peak due to the main crystalline phase of PVA; (3) the main melting peak area decreased exponentially with increasing W , and this indicated a reduction of X ; and (4) films with a CrF_3 W value greater than or equal to 10 wt % showed an additional melting peak, which indicated the presence of a dual structure. The X-ray analysis showed no significant peaks characterizing CrF_3 or MnCl_2 crystals. X of the main phase, detected by XRD, decreased exponentially with increasing W . It was observed that X could be used as a measure of W . Also, XRD confirmed the presence of two different crystalline phases for CrF_3 W values greater than or equal to 10 wt %, and this agreed with the DSC findings. Because of their similarity, the W dependence of the melting peak area and the corresponding dependence for the height of the main peak (101) confirmed each other. Therefore, it may be concluded that the crystalline structure changes in PVA due to filling depend on the chemical nature of the filling substances and the ways in which they interact with the host matrix. One may select a suitable type and W value of the filler to prepare a filled PVA films with a desired crystalline structure.

References

1. Tawansi, A.; Zidan, H. M.; Eldumiaty, A. H. *Polym Test* 1998, 17, 211.
2. Bahri, R. *J Phys D: Appl Phys* 1982, 15, 1036.
3. Nalwa, H. S. *J Mater Sci* 1992, 27, 210.
4. Tawansi, A.; Abdel-Razek, E. M.; Zidan, H. M. *J Mater Sci* 1997, 32, 6243.
5. Yamaura, K.; Kuranuki, N.; Suzuki, M.; Tanigami, T.; Matsuzawa, S. *J Appl Polym Sci* 1990, 41, 2409.
6. Ichimura, K. *J Polym Sci Polym Chem Ed* 1984, 22, 2817.
7. Hirai, T.; Asada, Y.; Suzuki, T.; Hayashi, S.; Nambu, M. *J Appl Polym Sci* 1989, 38, 491.
8. Hyon, S. H.; Cha, W. I.; Ikada, Y. *Kobunshi Ronbunshu* 1989, 46, 681.
9. Perepechko, I. I. *An Introduction to Polymer Physics*; Mir: Moscow, 1981; p 52.
10. Takahashi, Y. *J Polym Sci Part B: Polym Phys* 1997, 35, 193.
11. Tawansi, A.; Zidan, H. M.; Oraby, A. H.; Dorgham, M. E. *J Phys D: Appl Phys* 1998, 31, 3428.
12. Tawansi, A.; Oraby, A. H.; Zidan, H. M.; Dorgham, M. E. *Physica B* 1998, 254, 126.
13. Zidan, H. M. *Polym Test* 1999, 18, 449.
14. Mallapragada, S. K.; Peppas, N. A. *J Polym Sci Part B: Polym Phys* 1996, 34, 1339.
15. Garrett, P. D.; Grubb, D. T. *J Polym Sci Part B: Polym Phys* 1988, 26, 2509.
16. Nagura, M.; Matsuzawa, S.; Yamaura, K.; Ishikawa, H. *Polym Commun* 1983, 24, 250.
17. Popli, R.; Glotin, M.; Mandelkern, L.; Benson, R. S. *J Polym Sci Polym Phys Ed* 1984, 22, 407.
18. Gibbs, J. H. *Collected Works*; Longman Green: Essex, England, 1928.
19. Gregorio, R., Jr.; de Souza Nociti, N. C. P. *J Phys D: Appl Phys* 1995, 28, 432.
20. Cha, W.-I.; Hyon, S.-H.; Ikada, Y. *J Polym Sci Part B: Polym Phys* 1994, 32, 297.
21. Tanigami, T.; Nakashima, Y.; Murase, K.; Zuzuki, H.; Yamaura, K.; Matsuzawa, S. *J Mater Sci* 1995, 30, 5110.
22. Rijke, A. M.; Mandelkern, L. *J Polym Sci Part A-2: Polym Phys* 1970, 8, 225.
23. Bell, J. P.; Slade, P. E.; Dumbleton, J. H. *J Polym Sci Part A-2: Polym Phys* 1968, 6, 1773.
24. Hyon, S.-H.; Chu, H.-D.; Kiatmaru, R. *Bull Inst Chem Res Kyoto Univ* 1975, 53, 367.
25. Nagura, M.; Eisenberg, A. *Polymer* 1991, 32, 2205.
26. Mooney, R. C. L. *Proc Washington Meet Am Phys Soc* 1941, 63, 2828.
27. Gaafar, S. A.; Abd El-Kader, F. H.; Rizk, M. S. *Phys Scripta* 1994, 49, 366.
28. Das, P. S.; Adhikari, B.; Maiti, S. *J Polym Sci Part A: Polym Chem* 1994, 32, 39.